Defect modes properties in periodic lossy multilayer containing negative index materials with symmetric and asymmetric geometric structures

A. Aghajamali [1,2*] B. Javanmardi [3†], M. Barati [2‡], and C.-J. Wu [4§]

[1] *Young Researchers Club,*

Science and Research Branch,

Islamic Azad University, Fars, Iran

[2] *Department of Physics,*

Science and Research Branch,

Islamic Azad University, Fars, Iran

[3] *Department of Physics,*

Shahid Beheshti University,

G. C., Evin, Tehran 19839, Iran

[4] *Institute of Electro-Optical Science and Technology,*

National Taiwan Normal University,

Taipei 116, Taiwan, R.O.C.

Abstract

In this paper the characteristic matrix method is used to study the propagation of electromagnetic waves through one-dimensional lossy photonic crystals composed of negative and positive refractive index material layers with symmetric and asymmetric geometric structures with a defect layer at the center of the structure. First, the positive index material defect layer is considered, and the effects of the polarization and the angle of incidence on the defect mode in the transmission spectra of the both structures are investigated. The results show that the number of the defect modes in the transmission spectra depends on the geometry (symmetric or asymmetric) of the structure. In addition, it is shown that the defect mode frequency increases as the angle of incidence increases. This property is independent of the geometry of the structure. Then, for normal incidence, the negative index material defect layer is considered, and the properties of defect modes for both structures are investigated. The results can lead to designing new types of transmission narrow filters.

[*] email address: alireza.aghajamali@fsriau.ac.ir
[†] email address: behnam.javanmardi@gmail.com
[‡] email address: barati@susc.ac.ir
[§] email address: jasperwu@ntnu.edu.tw

I. INTRODUCTION

Photonic crystals (PCs) are artificial dielectrics or metallic structures in which the refractive index changes periodically. Due to their unique electromagnetic properties and important scientific and engineering applications, research on PCs has been an attractive topic in optics during past two decades [1–6]. The spatial periodicity of the PCs causes a range of forbidden frequencies called photonic band gap [7, 8]. The gap is formed as a result of Bragg scattering in a periodical dielectric structure through which no electromagnetic wave can propagate. By introducing a layer with different optical properties which breaks the periodicity of the PCs structure, localized defect modes will appear inside the band gap, very similar to the defect states that are generated in the forbidden band of doped semiconductors. The appearance of the defect modes is due to the change of the interference behavior of electromagnetic waves.

In 1967 Veslago [9] predicted the existence of materials with negative refractive index called metamaterials or Negative Index Materials (NIMs). NIM also known as left-handed material, has negative permittivity and permeability simultaneously. After experimental realization of metamaterials by Smith et al. [10], such materials have received extensive attention for their very unusual electromagnetic properties [11–17]. Recently, with the possibility of producing metamaterials, PCs with metamaterials, called metamaterial photonic crystals (MPCs) have been made. In 2003, Li et al. [18], have interestingly reported the appearance of an additional gap called zero-$\bar{n}$ gap in the transmission spectra of a one-dimensional (1D) PC composed of NIM and positive index material (PIM) dielectric layers.

In several papers the properties of the defect modes in different 1D conventional PC and 1D MPC structures are reported [19–34]. Following the interesting report by Wu et al. [24] on the properties of the defect modes in 1D conventional PC with symmetric and asymmetric structures, here we investigate the properties of the defect modes in the transmission spectra of 1D symmetric and asymmetric lossy MPCs structures with the defect layer at the center of the structure. First, we consider the PIM defect layer, and after that, the NIM defect layer has been considered.

The outline of this paper is as follows. In Section 2, two PMC structures, the permittivity and permeability of the NIM layer, and also the characteristic matrix method and its formulation are presented. The numerical computation and the results are given in Section 3, and the paper is concluded in Section 4.

II. MPC STRUCTURE AND CHARACTERISTIC MATRIX METHOD

A 1D MPC with asymmetric and symmetric structures in air with a defect layer at the center of the structure are shown in Figure 1a and Figure 1b, respectively. A is a NIM layer, B is a PIM layer, and defect layer C is either PIM or NIM. The NIM is assumed to be dispersive and dissipative. The permittivity and the permeability of layer A are complex, and are given by [18]:

$$\varepsilon_A(f) = 1 + \frac{5^2}{0.9^2 - f^2 - i\gamma f} + \frac{10^2}{11.5^2 - f^2 - i\gamma f} \tag{1}$$

$$\mu_A(f) = 1 + \frac{3^2}{0.902^2 - f^2 - i\gamma f} \tag{2}$$

where f and γ (given in GHz) are respectively frequency and damping frequency. Plots of the real parts of the permittivity and permeability of layer A, $\varepsilon_A^{'}$ and $\mu_A^{'}$, versus frequency for four different loss factors are shown in Figure 2. Also, more details of the various aspects $\varepsilon_A^{'}$ and $\mu_A^{'}$ have been discussed in our previous study [35].

Our calculation is based on the characteristic matrix method [36], which is the most effective method to analyze the transmission properties of PCs. In the absence of the defect layer, the characteristic matrix of the periodic structure $(AB)^N$ is given by:

$M[d] = (M_A M_B)^N$

where N is the number of the lattice periods. In the presence of the defect layer, the characteristic matrix for asymmetric $(AB)^{N/2}C(AB)^{N/2}$, and symmetric $(AB)^{N/2}C(BA)^{N/2}$ structures, respectively, are:

$M[d] = (M_A M_B)^{N/2} M_C (M_A M_B)^{N/2}$, and $M[d] = (M_A M_B)^{N/2} M_C (M_B M_A)^{N/2}$,

where M_A, M_B and M_C are the characteristic matrices of layers A, B, and C. The characteristic matrix M_i for TE waves at incidence angle θ_0 in vacuum is given by [36]:

$$M_i = \begin{bmatrix} \cos\gamma_i & \frac{-i}{p_i}\ \sin\gamma_i \\ -i\ p_i\ \sin\gamma_i & \cos\gamma_i \end{bmatrix} \tag{3}$$

where $\gamma_i = (\omega/c)\, n_i d_i \cos\theta_i$, c is speed of light in vacuum, θ_i is the angle of refraction inside the layer i with refractive index n_i and $p_i = \sqrt{\varepsilon_i/\mu_i}\ \cos\theta_i$, where $\cos\theta_i = \sqrt{1 - (n_0^2 \sin^2\theta_0/n_i^2)}$, in which n_0 is the refractive index of the environment where the incidence wave tends to enter the structure. The refractive index is given as $n_i = \pm\sqrt{\varepsilon_i \mu_i}$ [31, 37], where the positive and the negative signs are assigned for the PIM and NIM layers, respectively. The final characteristic matrix for an

N period structure is given by:

$$[M(d)]^N = \prod_{i=1,\ldots,N} M_i \equiv \begin{pmatrix} m_{11} & m_{12} \\ m_{21} & m_{22} \end{pmatrix} \tag{4}$$

where $m_{i,j}(i, j = 1, 2)$ are the matrix elements of $[M(d)]^N$. The transmission coefficient of the multilayer is calculated by:

$$t = \frac{2\ p_0}{(m_{11} + m_{12}\ p_s)\ p_0 + (m_{21} + m_{22}\ p_s)} \tag{5}$$

where $p_0 = n_0\ \cos\theta_0$ and $p_s = n_s\ \cos\theta_s$, with n_s being the refractive index of the environment where the wave leaves the crystal with angle θ_s. The transmissivity of the multilayer is given by

$$T = \frac{p_s}{p_0}|t|^2. \tag{6}$$

The transmissivity of the multilayer for TM waves can be obtained by using these previous expressions with $p_i = \sqrt{\frac{\mu_i}{\varepsilon_i}}\cos\theta_i$, $p_0 = \frac{\cos\theta_0}{n_0}$, and $p_s = \frac{\cos\theta_s}{n_s}$.

III. NUMERICAL RESULTS AND DISCUSSION

Based on the theoretical model described in the previous section, the transmission spectrum of the lossy MPC structures is calculated. In the first part, we use equations (1) and (2) for the permittivity and the permeability of layer A. Layers B and C are assumed to be PIM, and the refraction indices are $n_B = 1$ and $n_C = 2.7$. The thickness of layers A, B, and C are considered as $d_A = 6$ mm, $d_B = 12$ mm, and $d_C = 24$ mm. Calculations are performed with $N = 16$ [35] in the range of frequency where the zero-$\bar{n}$ gap appears [18, 35, 38, 39].

The transmission spectra of TE and TM polarized waves for the asymmetric structure at various angles of incidence and for $\gamma = 0.2 \times 10^{-3}$ GHz are shown in Figures 3 and 4, respectively. As it is seen, the defect layer causes two different modes. The modes are identified by numbers 1 and 2 in the figures. This is in sharp contrast to the report by Wu et al. [24] for the defect modes in 1D PCs with PIMs where only one defect mode for the asymmetric structure has been observed.

In this asymmetric 1D MPC, the frequency dependence of the defect modes as a function of the incidence angles for TE and TM waves and for $\gamma = 0.2 \times 10^{-3}$ GHz is illustrated in Figure 5. TE and TM modes start from the same value for zero incidence angle, as expected, but the starting points are different for different mode numbers. As the incidence angle increases, the frequency of the TM defect modes increases, but the frequency of the TE modes remains almost unchanged

for both defect modes. Similar behavior has been reported by Wu et al. [24] in the study of the symmetric PIM geometry structure. It is interesting to mention that the first TM defect mode disappears for an incidence angle greater than $\approx 50°$.

Now, the properties of the defect mode in the transmission spectrum of the 1D MPC with symmetric structure with a PIM defect layer at the center are investigated. The results for TE and TM polarized waves for different incidence angles and for $\gamma = 0.2 \times 10^{-3}$ GHz are shown in Figures 6 and 7, respectively. As it is seen from the figures, there exists only one defect mode in accordance with the work reported by Wu et al. [24] in the asymmetric structure.

The frequency dependence of the defect mode on the incidence angle for TE and TM waves is shown in Figure 8. It is seen that the frequency of the defect modes increase with a higher rate for TM wave were the incidence angle passes over $\approx 35°$.

In the last part, properties of the defect mode in the transmission spectra of both geometric structures with an NIM defect layer at the center and for normal incidence case are investigated. The asymmetric and symmetric structures which were used before are modified by replacing an NIM defect layer (layer C) in which the permittivity and permeability follow the equations (1) and (2), exactly like layer A. The other parameters are kept the same as the first part, PIM defect layer. The results of the asymmetric and symmetric structures for $\gamma = 0.2 \times 10^{-3}$ GHz are respectively shown in Figures 9(a) and 9(b). As it is seen, the NIM defect layer causes only one defect mode whose property is independent of the geometry of the structure. Moreover, the results show that the defect mode in the symmetric structure appears at a lower frequency compared to the asymmetric one. Furthermore, comparing the peak height of the defect modes in PIM and NIM defect layers shows that the peak height decreases when the NIM defect layer is considered.

IV. CONCLUSION

In this paper, the properties of defect modes coming from PIM and NIM defect layer at the center of a one-dimensional lossy MPC with symmetric and asymmetric structures on the transmission spectra have been investigated. Our numerical results show that defect modes with different characteristics for different geometries appear in the band gap. When the PIM defect layer is considered, there exists only one defect mode in the symmetric structure, but in the asymmetric structure two defect modes with different behaviors in the transmission spectra. Positions of the defect modes depend on the polarization of the waves and the incidence angles. As the incidence

angle increases the frequency of the defect modes moves toward higher frequencies regardless of the geometrical structure. Furthermore, one of the defect modes for TM polarized waves in the asymmetric structure disappears for incidence angles greater than . On the other hand, the results of the NIM defect layer show that only one defect mode which is independent of the geometric structure. Finally, an important result of this study is that by using a negative index material (metamaterial) in the structure of PCs, the defect modes show different behavior from the PCs with only positive index materials. In the latter conventional PCs case, as was mentioned earlier in the text, for a PIM defect layer, the symmetric geometric structure shows two defect modes and the asymmetric one shows one defect mode [24]. But in our case this is vice versa. Detailed analysis of the defect modes in metamaterial photonic crystals with symmetric and asymmetric structures will certainly provide useful information for designing new types of transmission narrow filters.

References

[1] Yablonovitch, E., "Inhibited spontaneous emission in solid-state physics and electronics," *Phys. Rev. Lett.*, Vol. 58, 2059-2062, 1987.

[2] John, S., "Strong localization of photons in certain disordered dielectric superlattices," *Phys. Rev. Lett.*, Vol. 58, 2486-2489, 1987.

[3] Noda, S., A. Chutinan, and M. Imada, "Trapping and emission of photons by a single defect in a photonic bandgap structure," *Nature*, Vol. 407, 608-610, 2000.

[4] Massaoudi, S., A. de Lustrac, and I. Huynen, "Properties of metallic photonic band gap material with defect at microwave frequencies: calculation and experimental verification," *J. Electromagn. Waves Appl.*, Vol. 14, 1967-1980, 2006.

[5] Mandal, B. and A. R. Chowdhury, "Spatial soliton scattering in a quasi phase matched quadratic media in presence of cubic nonlinearity," *J. Electromagn. Waves Appl.*, Vol. 1, 123-135, 2007.

[6] Zheng, Q. R., B. Q. Lin, and N. C. Yuan, "Characteristics and applications of a novel compact spiral electromagnetic band-gap (EBG) structure," *J. Electromagn. Waves Appl.*, Vol. 2, 199-213, 2007.

[7] Yablonovitch, E., "Photonic band structure: the face-centered-cubic case employing nonspherical atoms," *Phys. Rev. Lett.*, Vol. 67, 2295-2298, 1991.

[8] Joannopoulos, J. D., S. G. Johnson, J. N. Winn, and R. D. Meada, *Photonic crystals: Modeling the flow of light*, Princeton University Press, Princeton, 2008.

[9] Veselago, V. G., "The electrodynamics of substances with simultaneously negative values of ε and μ," *Sov. Phys. Usp.*, Vol. 10, 509-514, 1968.

[10] Smith, D. R., W. J. Padilla, D. C. Vier, S. C. Nemat-Naser, and S. Schuitz, "Composite medium with simultaneously negative permeability and permittivity," *Phys. Rev. Lett.*, Vol. 84, 4184-4187, 2000.

[11] Engheta, N. and R. W. Ziolkowski, *Metamaterials: Physics and engineering explorations*, John Wiley & Sons, New Jersey, 2006.

[12] Caloz, C. and T. Itoh, *Electromagnetic metamaterials: Transmission line theory and microwave applications*, John Wiley & Sons, New Jersey, 2006.

[13] Cai, W. and V. Shalaev, *Optical metamaterials: Fundamentals and applications*, Springer, New York, 2010.

[14] Eleftheriades, G. V. and K. G. Balmain, *Negative refraction metamaterials: Fundamentals properties and applications*, John Wiley & Sons, New Jersey, 2005.

[15] Novitsky, A. V. and L. M. Barkovsky, "Guided modes in negative-refractive-index fibres," *J. Opt. A Pure Appl. Opt.*, Vol. 7, S51-S56, 2005.

[16] Cory, H. and T. Blum, "Surface-wave propagation along a metamaterial cylindrical guide," *Microw. Opt. Technol. Lett.*, Vol. 44, 31-35, 2005.

[17] Kim, K. Y., J. H. Lee, Y. K. Cho, and H. S. Tae, "Electromagnetic wave propagation through doubly dispersive subwavelength metamaterial hole," *Opt. Express*, Vol. 13, 3653-3665, 2005.

[18] Li, J., L. Zhou, C. T. Chan, and P. Sheng, "Photonic band gap from a stack of positive and negative index materials," *Phys. Rev. Lett.*, Vol. 90, 083901-083904, 2003.

[19] Lotfi, E., K. Jamshidi-Ghaleh, F. Moslem, and H. Masalehdan, "Comparison of photonic crystal narrow filters with metamaterials and dielectric defects," *Eur. Phys. J. D*, Vol. 60, 369-372, 2010.

[20] Zhu, Q. and Y. Zhang, "Defect modes and wavelength tuning of one-dimensional photonic crystal with lithium niobate," *Optik*, Vol. 120, 195-198, 2009.

[21] Abdel-Rahman, E. and A. Shaarawi, "Defect mode in periodic and quasiperiodic one-dimensional photonic structures," *J Mater Sci: Mater Electron*, Vol. 20, S153-S158, 2009.

[22] Ansari, N., M. M. Tehranchi, and M. Ghanaatshoar, "Characterization of defect modes in one-dimensional photonic crystals: An analytic approach," *Physica B*, Vol. 404, 1181-1186, 2009.

[23] Li, X., K. Xie, and H. M. Jiang, "Properties of defect modes in one-dimensional photonic crystals containing two nonlinear defects," *Opt. Commun.*, Vol. 282, 4292-4295, 2009.

[24] Wu, C. -J. and Z. H. Wang, "Properties of defect modes in one-dimensional photonic crystals," *Progress In Electromagnetics Research*, Vol. 103, 169-184, 2010.

[25] Ansari, N. and M. M. Tehranchi, "Influence of filling fraction on the defect mode and gap closing of a one-dimensional photonic crystal: An analytical approach," *Physica B*, Vol. 405, 2900-2906, 2010.

[26] Gharaati, A. and H. Azarshab, "Characterization of defect modes in one-dimensional ternary metallo-dielectric nanolayered photonic crystal," *Progress In Electromagnetics Research B*, Vol. 37, 125-141, 2012.

[27] Zhang, W., P. Han, A. Lan, Y. Li, and X. Zhang, "Defect modes tuning of one-dimensional photonic crystals with lithium niobate and silver material defect," *Physica E*, Vol. 44, 813-815, 2012.

[28] Aly, A. H. and H. A. Elsayed, "Defect mode properties in a one-dimensional photonic crystal," *Physica B*, Vol. 407, 120-125, 2012.

[29] Chen, Y. H., G. Q. Liang, J. W. Dong, and H. Z. Wang, "Derivation and characterization of dispersion of defect modes in photonic band gap from stacks of positive and negative index materials," *Phys. Lett. A*, Vol. 351, 446-451, 2006.

[30] Kang-Song, T., X. Yuan-Jiang, and W. Shuang-Chun, "Defect in photonic crystal with negative index material," *Optoelectron. Lett.*, Vol. 2, 118-121, 2006.

[31] Jiang, H., H. Chen, H. Li, and Y. Zhang, "Omnidirectional gap and defect mode of one-dimensional photonic crystals containing negative-index materials," *Appl. Phys. Lett.*, Vol. 83, 5386-5388, 2003.

[32] Wang, L. G., H. Chen, and S. Y. Zhu, "Omnidirectional gap and defect mode of one-dimensional photonic crystals with single-negative materials," *Phys. Rev. B*, Vol. 70, 245102-245107, 2004.

[33] Xu, Q., K. Xie, H. Yang, and J. Tang, "Periodic defect modes of one-dimensional crystals containing single-negative materials," *Optik*, Vol. 121, 1558-1562, 2010.

[34] Xiang, Y., X. Dai, S. Wen, and D. Fan, "Properties of omnidirectional gap and defect mode of one-dimensional photonic crystal containing indefinite metamaterials with a hyperbolic dispersion," *J. Appl. Phys.*, Vol. 102, 093107-093111, 2007.

[35] Aghajamali, A. and M. Barati, "Effects of normal and oblique incidence on zero-$\bar{n}$ gap in periodic lossy multilayer containing double-negative materials," *Physica B*, Vol. 407, 1287-1291, 2012.

[36] Born, M. and E. Wolf, *Principles of Optics: Electromagnetic theory of propagation, Interference and diffraction of light*, Cambridge University Press, UK, 2005.

[37] Zhang, L., Y. Zhang, L. He, Z. Wang, H. Li, and H. Chen, "Zero-$\bar{n}$ gaps of photonic crystals consisting of positive and negative index materials in microstrip transmission lines," *J. Phys. D: Appl. Phys.*, Vol. 40, 2579-2587, 2007.

[38] Daninthe, H., S. Foteinopoulou, C. M. Soukoulis, "Omni-reflectance and enhanced resonant tunneling from multilayers containing left-handed materials," *Photoni. Nanostruct.*, Vol. 4, 123-131, 2006.

[39] Awasthi, S. K., A. Mishra, U. Malaviya, and S. P. Ojha, "Wave propagation in a one-dimensional photonic crystal with metamaterial," *Solid State Commun.*, Vol. 149, 1379-1383, 2009.

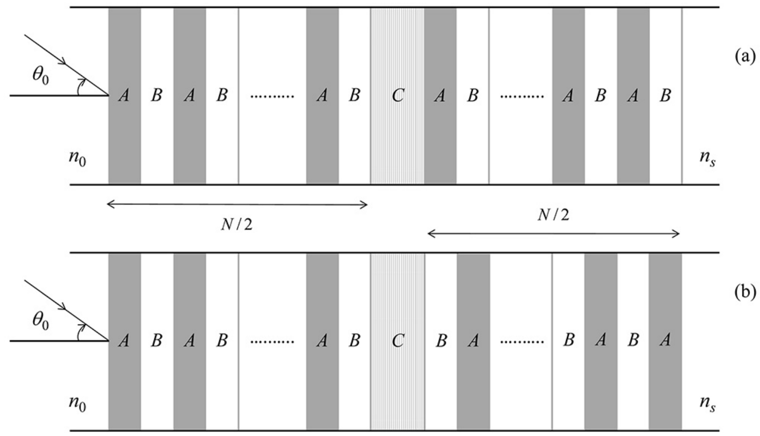

FIG. 1: Schematic diagrams of 1D MPCs which are embedded in air, with a defect layer, (a) asymmetric structure, (b) symmetric structure, where layer A is the NIM and layer B is PIM. The number of the periods is N and the incidence angle is θ_0.

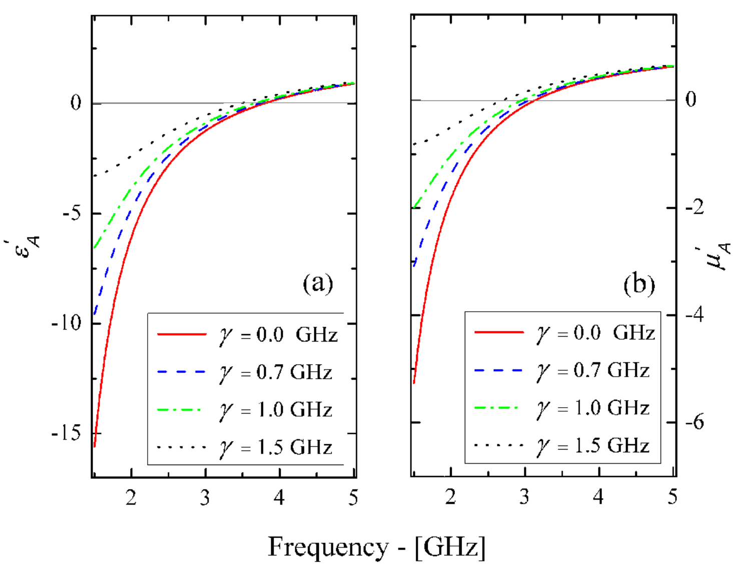

FIG. 2: Real parts of (a) the permittivity and (b) the permeability of layer A, $\varepsilon_A^{'}$ and $\mu_A^{'}$, versus frequency for $\gamma = 0$, 0.7, 1, and 1.5 GHz.

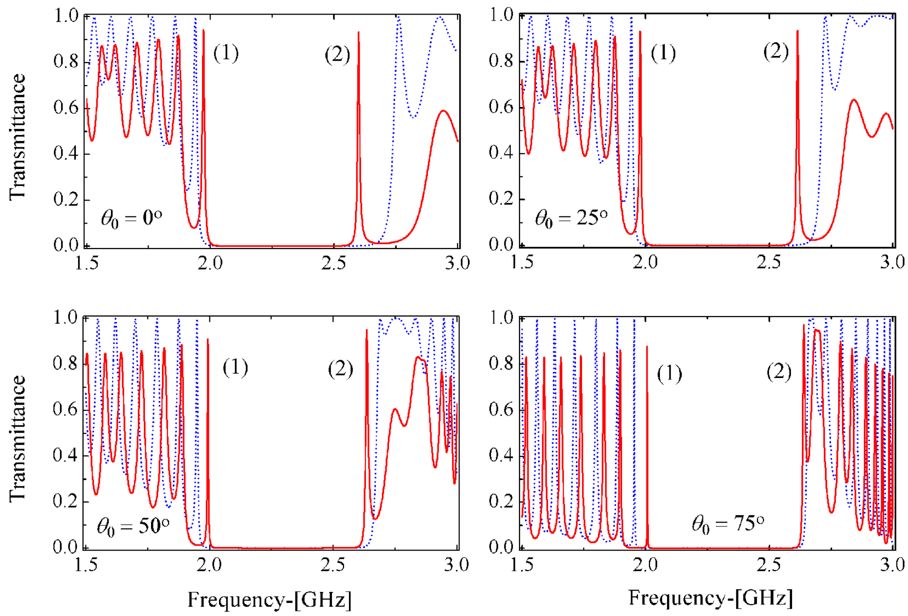

FIG. 3: Transmission spectra of TE polarized wave for the asymmetric 1D MPC structures with PIM defect layer (solid line) and without defect layer (dotted line) for different incidence angles with $\gamma = 0.2 \times 10^{-3}$ GHz.

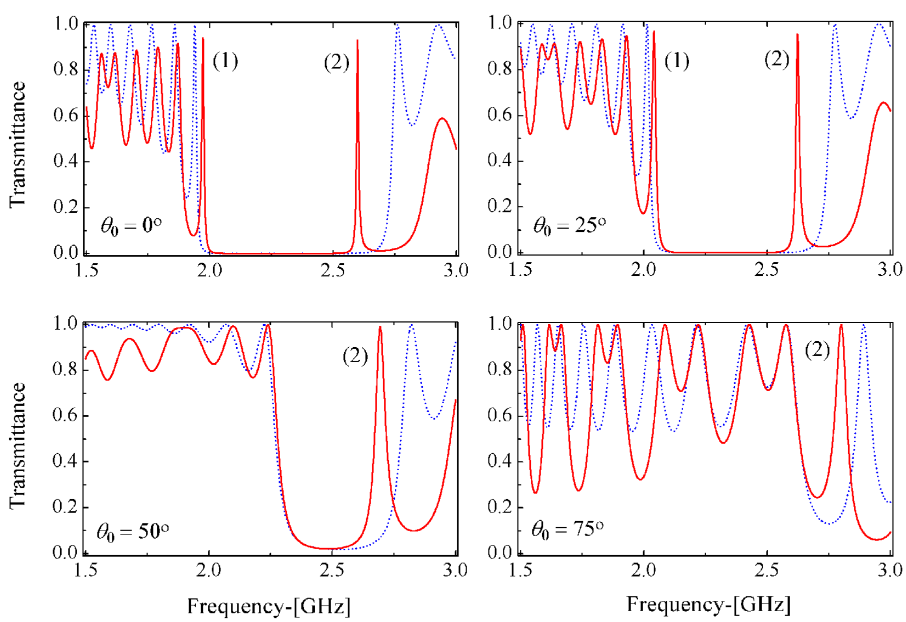

FIG. 4: Transmission spectra of TM polarized wave for the asymmetric 1D MPC structures with PIM defect layer (solid line) and without defect layer (dotted line) for different incidence angles with $\gamma = 0.2 \times 10^{-3}$ GHz.

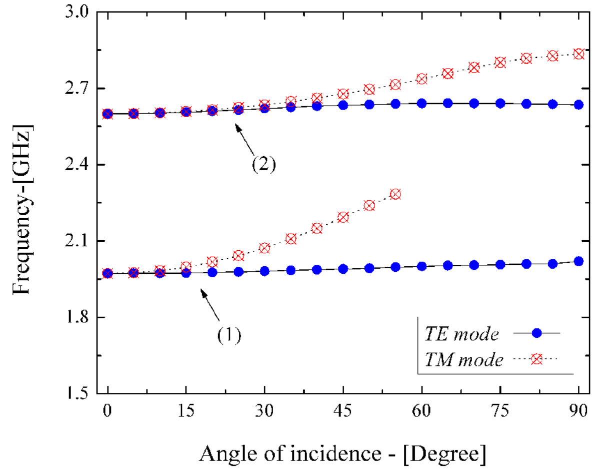

FIG. 5: Frequency of the defect modes in the asymmetric 1D PMC as a function of angle of incidence for both polarizations, with $\gamma = 0.2 \times 10^{-3}$ GHz.

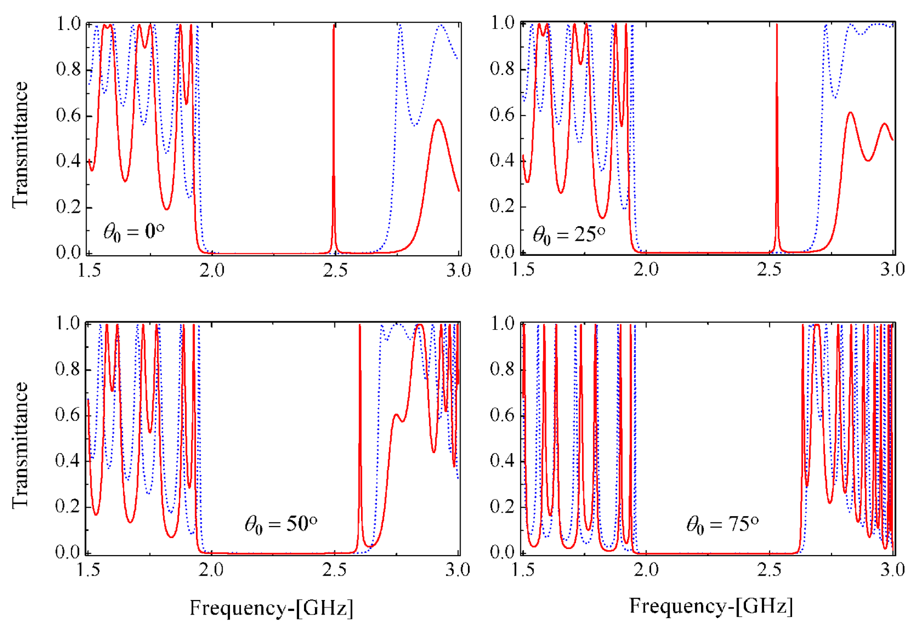

FIG. 6: Transmission spectra of TE polarized wave for the symmetric 1D MPC structures with PIM defect layer (solid line) and without defect layer (dotted line) for different incidence angles with $\gamma = 0.2 \times 10^{-3}$ GHz.

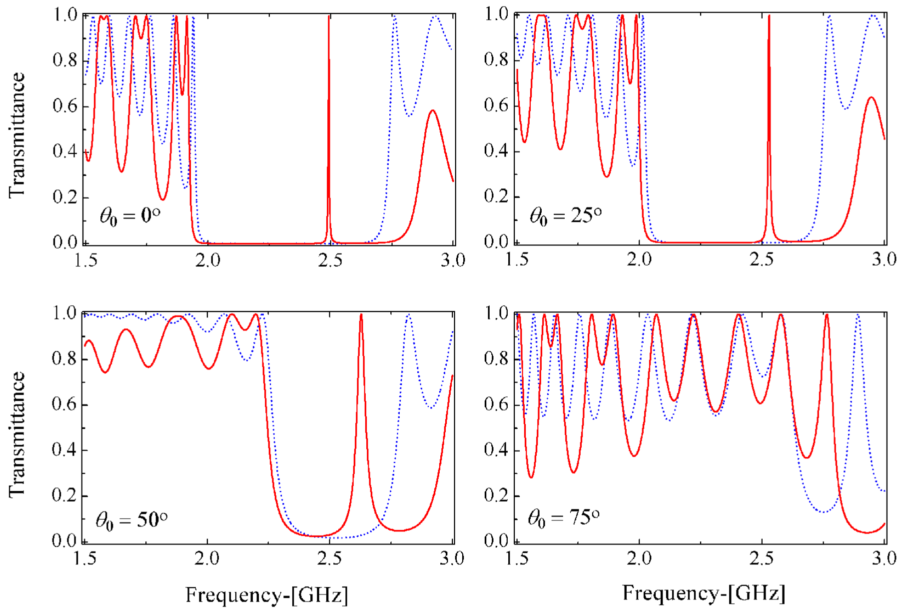

FIG. 7: Transmission spectra of TM polarized wave for the symmetric 1D MPC structures with PIM defect layer (solid line) and without defect layer (dotted line) for different incidence angles with $\gamma = 0.2 \times 10^{-3}$ GHz.

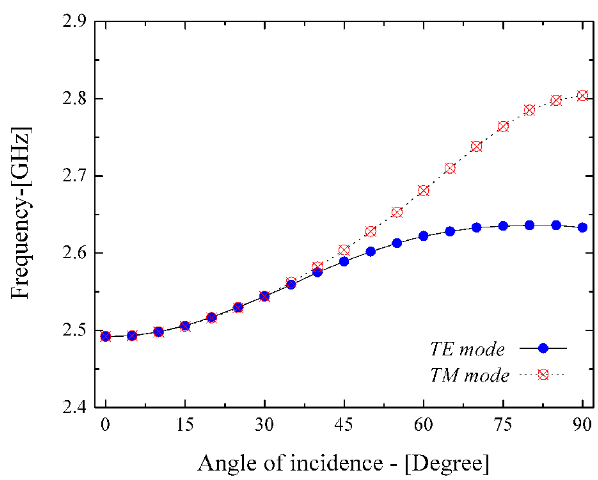

FIG. 8: Frequency of the defect modes in the symmetric 1D PMC as a function of angle of incidence for both polarizations, with $\gamma = 0.2 \times 10^{-3}$ GHz.

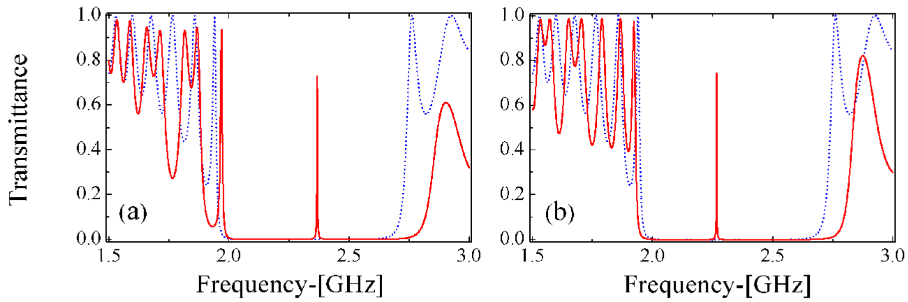

FIG. 9: Transmission spectra of (a) asymmetric and (b) symmetric 1D MPC structures with NIM defect layer (solid line) and without defect layer (dotted line) for normal incidence angle with $\gamma = 0.2 \times 10^{-3}$ GHz.